

# DEUTSCHES ELEKTRONEN-SYNCHROTRON **DESY**

DESY SR 85-05  
April 1985

ELECTRON-ENERGY-LOSS X-RAY ABSORPTION SPECTROSCOPY:  
A NON-DESTRUCTIVE STRUCTURAL-DEPTH-MICROPROBE

by

M.J. Bedzyk, G. Materlik

*Hamburger Synchrotronstrahlungslabor HASYLAB at DESY*

Eigentum der Property of	<b>DESY</b>	Bibliothek library
Zugang: Accessions:	28. JUNI 1985	
Leihfrist: Loan period:	7	Tage days

ISSN 0723-7979

NOTKESTRASSE 85 · 2 HAMBURG 52

DESY behält sich alle Rechte für den Fall der Schutzrechtserteilung und für die wirtschaftliche Verwertung der in diesem Bericht enthaltenen Informationen vor.

DESY reserves all rights for commercial use of information included in this report, especially in case of filing application for or grant of patents.

To be sure that your preprints are promptly included in the  
HIGH ENERGY PHYSICS INDEX ,  
send them to the following address ( if possible by air mail ) :

DESY  
Bibliothek  
Notkestrasse 85  
2 Hamburg 52  
Germany

Electron-Energy-Loss X-Ray Absorption Spectroscopy:  
a Non-Destructive Structural-Depth-Microprobe

M.J. Bedzyk\* and G. Materlik

Hamburger Synchrotronstrahlungslabor HASYLAB, DESY,  
Notkestr. 85, D-2000 Hamburg 52, Germany

Abstract

A simple gas-flow proportional counter was used to measure X-ray absorption spectra by registration of electrons emitted from a sample which was placed inside the volume of the counter. The sample volume was analysed in depth, layer-by-layer, by detecting the emitted electrons in an energy dispersive manner. This is demonstrated for a mixed-valent SmS crystal sample which was oxidized in a region close to the surface.



PACS numbers: 78.70.Dm, 71.50.+t, 79.60.-1

submitted for publication in Phys. Rev. B

X-ray absorption spectroscopy (XAS) has been a valuable tool over the past decade for obtaining important information concerning the structure and the electronic states of atoms in different environments<sup>1</sup>. Extended X-ray absorption fine structure (EXAFS)<sup>2</sup>, as well as, X-ray absorption near edge structure (XANES)<sup>3</sup> analysis have been carried out by measuring either the transmitted intensity relative to the incident beam, or by registration of fluorescence or electron-emission yields. Fluorescence lines and Auger electrons, which are characteristic for a specific atom, have been favourably used for increasing the signal-to-noise ratio, thus improving the sensitivity for elements in diluted samples. Even surface adsorbates can be studied by using the electron yield<sup>4</sup>. An instructive comparison for different electron detection modes, such as total, elastic Auger, partial Auger, or secondary electron yield, is given by Stöhr et al<sup>5</sup>.

Recently, it has also been demonstrated that gas-flow proportional counters can be used for conversion electron Mößbauer spectroscopy (CEMS)<sup>6</sup>, for X-ray standing-wave analysis<sup>7</sup>, and for EXAFS<sup>8</sup>. This electron detection scheme, which avoids the need for placing the sample in an evacuated volume, is implemented by placing the sample inside the gas-volume of the detector and collecting the integral electron yield at the anode wire. Such a registration contains information integrated over the escape-depth of the electrons. As pointed out in ref. 8, the measurement of electrons is advantageous in XAS when thick-diluted samples are studied. The photon fluorescence detection, under these circumstances, can become unfavourable, because a decrease of the absorption coefficient causes an increase of the penetration-depth of the primary photon. This increases the fluorescence yield and simulates an increase of the absorption coefficient.

Whereby the measured fluorescence yield EXAFS curve loses its characteristic structures. Since the electron escape-depth is usually small<sup>7</sup>, the change in the penetration-depth of the primary photon is not reflected in the yield curve. This is also the case, if low energy fluorescence photons with small absorption lengths are detected.

In contrast to fluorescence photons, however, electrons lose an appreciable part of their kinetic energy on their way out of the sample by inelastic scattering (with other electrons and plasmons for example). Electrons, originating from deeper inside the sample, leave the surface with a smaller energy than those being created with the same amount of kinetic energy by a photon absorption process happening close to the sample surface. As demonstrated for the case of CEMS<sup>9</sup> and for X-ray standing-wave analysis<sup>7</sup>, a depth sensitivity can be realized by the energy-dispersive registration of the electron yield.

The present study reports the successful application of a proportional counter to reach such a depth sensitivity also for XAS measurements. Such a development is important for XAS studies of multilayer structures, as well as for studies of samples which might contain a non-stoichiometric distribution of atoms as a function of the depth below the surface. As an example, we have chosen a SmS single crystal whose surface region was partly oxidized, and have measured the Sm L<sub>3</sub> absorption edge. Since Sm has a different valence state in pure and oxidized SmS<sup>10</sup>, this difference should show up in an electron-energy-loss XANES measurement.

We have used the ROEMO instrument<sup>11</sup> at the Hamburg Synchrotron Radiation

Laboratory HASYLAB at DESY in Hamburg. The experimental layout is shown in Fig. 1. Synchrotron radiation from the storage ring DORIS, running at 3.7 GeV with a medium electron current of 70mA, was monochromatized by a Si(111) double crystal monochromator. The first crystal was cut asymmetrically to condense the photon beam and to allow for easy detuning of the harmonics by operating at 90% of the maximum reflectivity<sup>11</sup>. The energy calibration was done relative to the Cu K edge. A small and constant energy window of 1 eV (at 6.7 keV) was provided by installing the first 1.0 mm slit at 7 m from the source (which had a typical height of 1.5 mm at this electron energy). The second 1 mm slit, placed in front of I<sub>0</sub>, was 0.1 x 0.1 mm<sup>2</sup>. Ion chamber I<sub>m</sub> was used to monitor the monochromator reflectivity and I<sub>0</sub> was used to measure the flux incident on the SmS sample which was placed inside the proportional counter<sup>12</sup>. A mixture of 90% He and 10% methane was used as flow-gas for the e<sup>-</sup> counter. The output from the anode wire went via a preamplifier into a spectroscopy amplifier set at a shaping time of 0.25 μsec.

Figure 2 shows two electron-emission spectra recorded at two different photon energies, just below the Sm L<sub>3</sub> edge and right on the top of the Sm 2+ white line. A signal from a random-pulse-generator (RP) was used to correct for deadtime losses. These spectra are accordingly normalized to the total counts in I<sub>0</sub> and to the RP signal per real time. The difference between the spectra is due to the additional creation of a Sm 2p<sup>3/2</sup> hole at photon energies larger than the 2p<sup>3/2</sup> binding energy. The nonradiative decay of this state creates L<sub>3</sub>-XY Auger electrons which have an initial kinetic energy > 3.27 keV. Their yield is given by the difference between the spectra shown in Fig. 2. An L<sub>3</sub>-XY Auger electron, originating from close to the surface, will be detected in the high-energy part of this spectrum. An electron originating (with the same

initial energy) from deep in the sample, will contribute to the low-energy region.

Different energy windows A, B, and C (Fig. 2) were selected by a single-channel-analyser and the intensity in each energy window was measured subsequently as a function of photon energy. These spectra are shown in Fig. 3 after subtraction of a linear background. Part C clearly exhibits two white lines which are characteristic for the different valence states<sup>13</sup> of the Sm atom in SmS ( $4f^6, (5d6s)^2$ ) and in Sm<sub>2</sub>O<sub>3</sub> ( $4f^5, (5d6s)^3$ ), and are described as 2+ and 3+ states, respectively. Going from A to C one clearly notices the change of the relative height of the valence states. Electrons contributing to C have lost a much smaller amount of energy than those in B and the same relation holds from B to A. C-electrons thus originate from a near-surface-region where the oxygen content is higher than in B. While most of the A-electrons are excited from deep inside the crystal ( $> 1000 \text{ \AA}$ ), in a region which has not been oxidized.

The solid lines in Fig. 3 are results of  $\chi^2$ -fits to a theoretical model which approximates the near-edge-region of each valence state by one Lorentzian for the  $2p^{3/2} \rightarrow 5d$  transition and by an additional arc tangent curve for transitions into continuum-like higher states<sup>14</sup>. This composition, convoluted with the experimental window function and with the life-time broadening, is shown in part C of Fig. 3.

The Lorentzians are centered at  $E_{L2}$  and  $E_{L3}$  and the inflection points of the arc tangent curves are at  $E_{AT2}$  and  $E_{AT3}$ . The best  $\chi^2$ -fit was determined in

A, B, and C for  $E_{L3} - E_{L2} = E_{AT3} - E_{AT2} = 7.5 \text{ eV}$  with a width (FWHM) of 5.2 eV. Case A was used to find the values for  $E_{L2} - E_{AT2} = E_{L3} - E_{AT3} = 0 \text{ eV}$  and for the ratio of 1.70 for the maximum of the Lorentzian to the height of the connected arc tangent curve. The results of the  $\chi^2$ -fits show that the ratio of the Sm<sup>3+</sup> content increases from 14.7 to 22.1 to 30.0% when going from A to B to C. This clearly reflects the increasing oxide content when going towards the surface from the inside of the SmS crystal.

It is useful to compare the result of the electron emission case to a spectrum measured in transmission with a powdered sample of pure SmS<sup>15</sup> shown in Fig. 4. In using the same  $\chi^2$ -fit procedure, as used for the e<sup>-</sup> emission spectra, the best fit gives other values for the width of the Lorentzian (5.67 eV) and for the ratio of the maximum of the Lorentzian to the jump of the arc tangent curve (1.40). The shoulder on the high-energy-side of the white line simulates a mixture of 8.4% 3+-valent Sm. However, since this sample was pure SmS, this shoulder is most likely characteristic for the Sm absorption edge in SmS. Therefore, this 8.4% should be subtracted from the other values given for A to C, when the additional oxidized part is determined.

It is interesting to note that the strength of the white line (as characterized by the product of Lorentzian height \* Lorentzian width) of the purest electron spectrum A is larger than that of the transmission case. This difference is up to 10% when the height of the white line of A is corrected for the reduction of 6.3% from the oxygen content. This discrepancy can be caused by the difference of sample thicknesses which contribute to the

measured signal in either case. This points to another possible advantage for using electrons instead of measuring XAS in the transmission mode. The spectra are much less affected by the thickness effect<sup>16</sup> which allows for a more direct comparison to theoretical calculations.

In conclusion, we have demonstrated that a simple gas-flow-proportional counter can be used to measure X-ray absorption spectra in a depth-sensitive manner. If needed, the resolution of this detector can still be improved or other e<sup>-</sup> detection schemes can be considered. This method samples the crystal layer-by-layer<sup>17</sup> and the electron collection is done very efficiently over a wide solid angle so that very small spot sizes are sufficient for detection. It therefore makes the application, as a 3-dimensional structural microprobe, easy. For example, the very simple design of the detector makes it possible to characterize sample surface-layers used for other applications and also to study reactions on surfaces.

We would like to thank Dr. K.-H Frank for the loan of the SmS crystal and Dr. B. Lengeler for providing the spectrum of the pure SmS sample.

#### References

\*Present address: Cornell High Energy Synchrotron Source (CHESS) and the School of Applied and Engineering Physics, Cornell University, Ithaca, New York 14853.

1. E.A. Stern and S.M. Heald in Handbook on Synchrotron Radiation, Vol. 1b, ed. by E.E. Koch, North-Holland Publ. Comp., 955 (1983).
2. B.K. Teo and D.C. Joy, EXAFS Spectroscopy, Plenum Press (1980).
3. EXAFS and Near Edge Structure, eds. A. Bianconi, L. Incocchia and S. Stipcich, in Springer Series in Chemical Physics 27, (1983).
4. P.H. Citrin and J.E. Rowe, Surf. Sci. 132, 205 (1983).
5. J. Stöhr, C. Noguera and T. Kandlewicz, Phys. Rev. B30, 5571 (1984).
6. K.R. Swanson and J.J. Spijkerman, J. Appl. Phys. 41, 3155 (1970).
7. M.J. Bedzyk, G. Materlik and M.V. Kovalchuk, Phys. Rev. B30, 4881 (1984).
8. M.E. Kordesch and R.W. Hoffmann, Phys. Rev. B29, 491 (1984).
9. G.N. Belozerskii, C. Bohm, T. Ekdahl and D. Liljequist, Nucl. Instr. and Meth. 192, 539 (1982).
10. G. Krill, J.P. Kappler, J. Röhlér, M.F. Ravet, J.M. Léger and F. Gautier in Valence Instabilities, eds. P. Wachter and H. Boppert, North-Holland Publ. Comp., 155 (1982).

11. A. Krolzig, G. Materlik, M. Swars and J. Zegenhagen, Nucl. Instr. and Meth. 219, 430 (1984).
12. N. Hertel, M.V. Kovalchuk, A.M. Afanasev and R.M. Imamov, Phys. Lett. 75A, 501 (1980).
13. G. Materlik, B. Sonntag and M. Tausch, Phys. Rev. Lett. 51, 1300 (1983).
14. We are aware that this model is only a coarse approximation. However, this is sufficient for the present purpose.
15. This spectrum was measured by B. Lengeler using the same spectrometer.
16. L.G. Paratt, C.F. Hempstead and E.L. Jossem, Phys. Rev. 105, 1228 (1957).
17. The stopping profiles of keV electrons in some solids were calculated by S. Valkealahti and R.M. Nieminen, Appl. Phys. A32, 95 (1983) and can serve to estimate the feasible spatial resolution.

#### Figure Captions

- Figure 1 Schematic experimental arrangement (for details see text).
- Figure 2 Electron spectra recorded with the proportional counter at two different photon energies  $E_f$ . Note, that the energy resolution of the detector has not been optimized for this measurement (for details see text).
- Figure 3 SmS XANES spectra measured with electron energy regions A, B, and C (see Fig. 2) at the Sm  $L_3$ -edge (for details see text).
- Figure 4 SmS XANES spectrum measured in transmission geometry at the Sm  $L_3$ -edge.

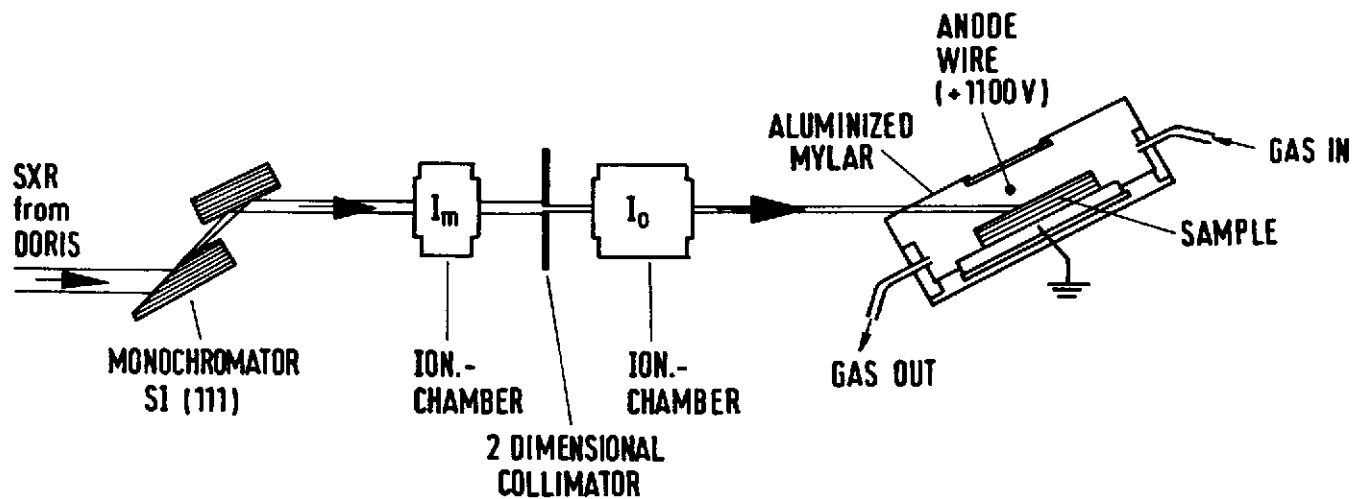


Fig. 1

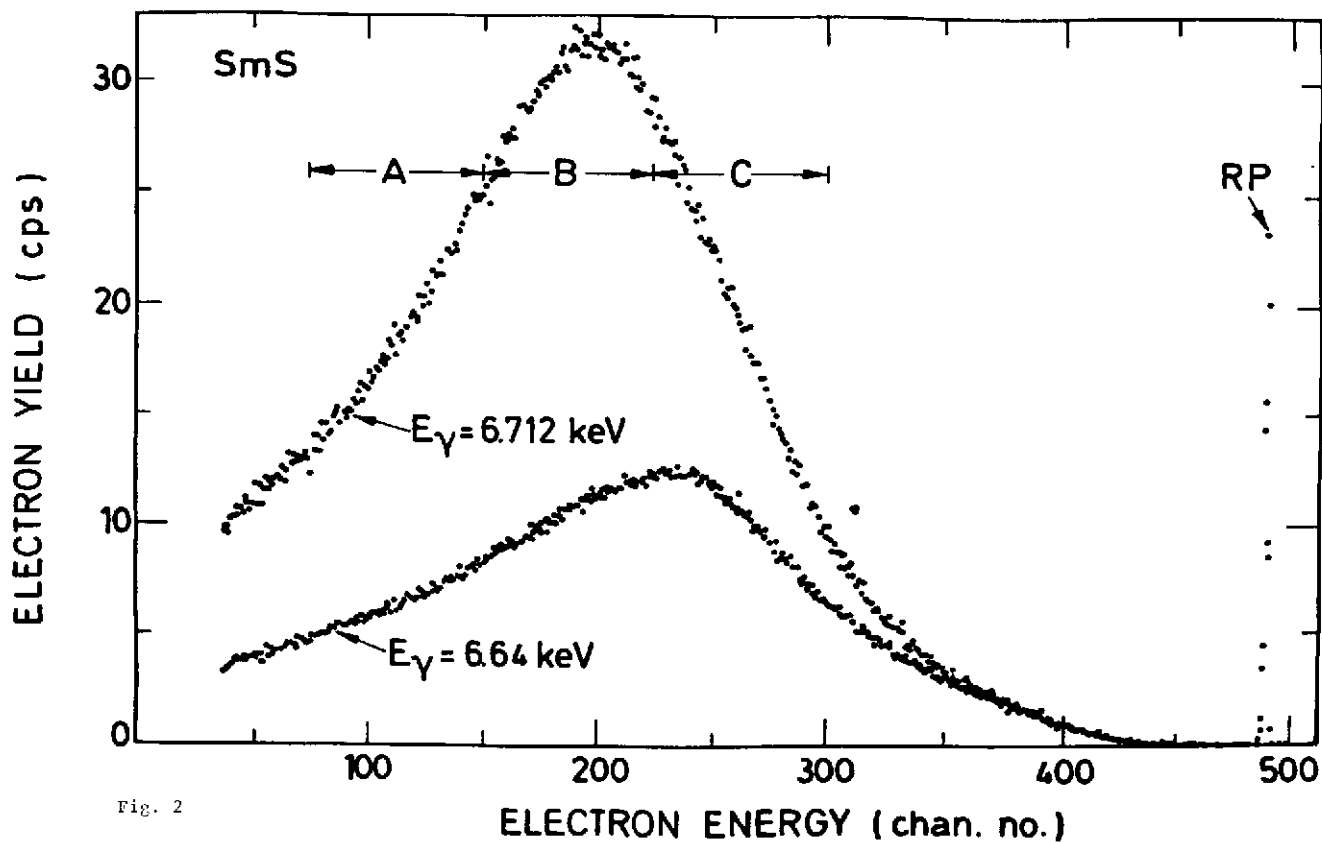


Fig. 2



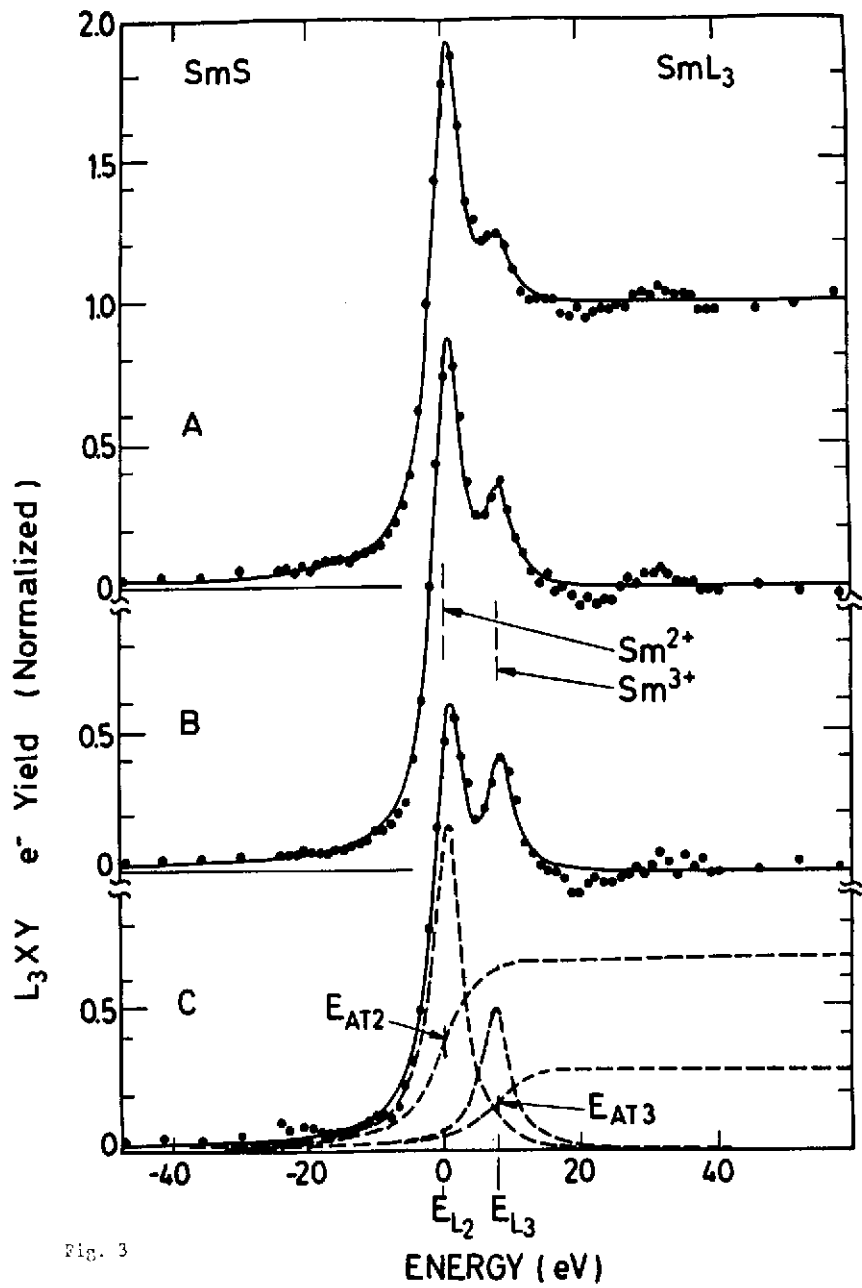


Fig. 3

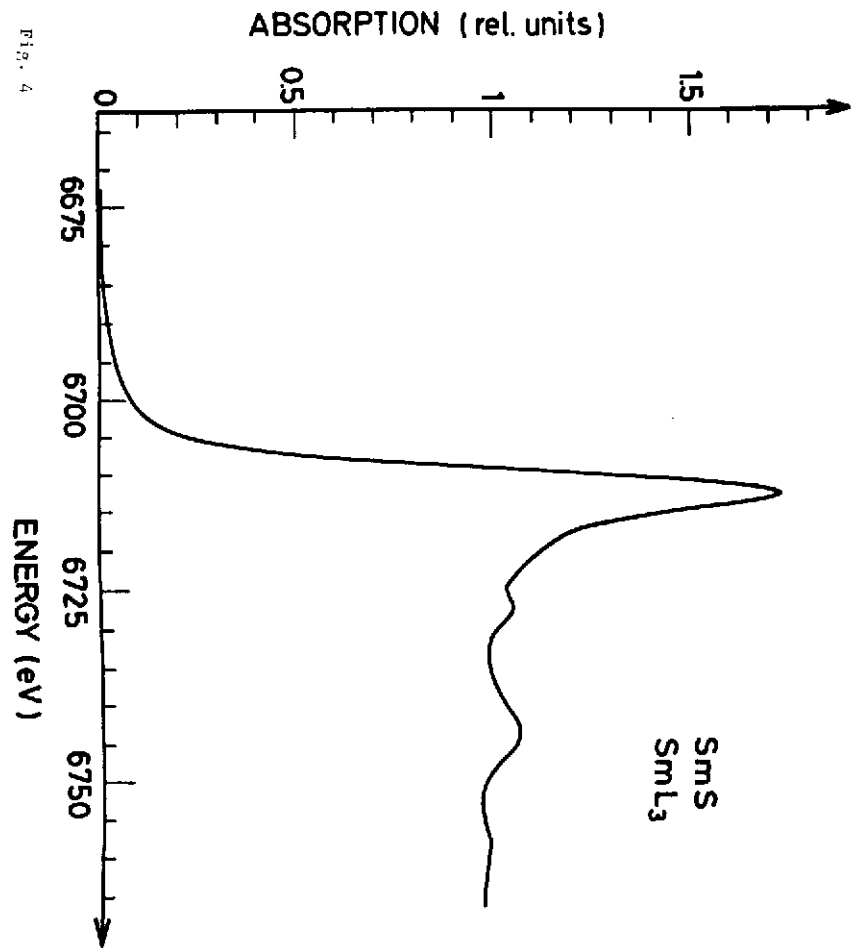


Fig. 4

